

Relevance-Guided Modeling of Object Dynamics for Reinforcement Learning

William Agnew Pedro Domingos

University of Washington
{wagnew3, pedrod}@cs.washington.edu

Abstract

Current deep reinforcement learning approaches incorporate minimal prior knowledge about the environment, limiting computational and sample efficiency. Objects provide a succinct and causal description of the world, and several recent works have studied unsupervised object representation learning using priors and losses over static object properties like visual consistency. However, object dynamics and interaction are critical cues for objectness. In addition, extensive research has shown humans have a working memory limited to only a small number of task relevant objects. In this paper we propose a framework for reasoning about object dynamics and behavior to rapidly determine minimal and task-specific object representations. We show the need for this reasoning over object behavior and dynamics by introducing a suite of RGBD MuJoCo object collection and avoidance tasks that, while intuitive and visually simple, confound state of the art unsupervised object representation learning algorithms. We also demonstrate the potential of this framework on a number of Atari games, using our object representation and standard RL and planning algorithms to learn over 10,000x faster than standard deep RL algorithms, and faster even than human players.

Introduction

Deep reinforcement learning has achieved impressive performance in many environments (Mnih et al. 2015, 2016; Silver et al. 2017). However, the sample inefficiency of deep reinforcement learning algorithms limits applicability to real-world domains. In addition, learned policies lack robustness to changes in visual inputs. These algorithms are very general, in theory capable of learning in all environments. We are only interested in real-world environments though, suggesting that current deep reinforcement learning algorithms could be improved by incorporating additional priors or heuristics.

In most real-world environments, humans are able to achieve good performance after far less experience than machines, pointing to human-inspired priors as a means of improving sample efficiency. Past work has considered perceiving the world in terms of objects as humans do ((Diuk, Cohen, and Littman 2008; Scholz et al. 2014)), and recent

work has focused on creating object state representations without supervision (Zhu, Huang, and Zhang 2018; Greff et al. 2019; Lin et al. 2020; Du et al. 2020). In this paper, we use human object priors to motivate a framework for reasoning about object dynamics and behavior to rapidly determine minimal and task-specific object representations. In addition, we propose a flexible reinforcement learning architecture that incorporates the prior that objects only act on each other when in contact to greatly improve sample efficiency and robustness.

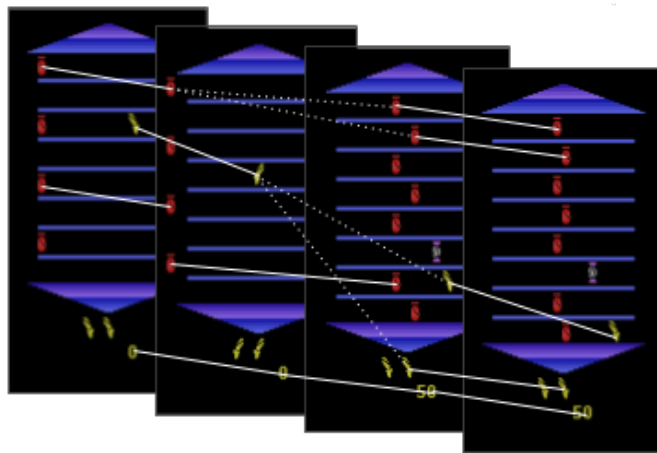


Figure 1: Tracklets (while lines) over percepts and proposed tracklet merges (dotted white lines) over four successive environment observations. Our object representation objective scores proposed tracklet merges, allowing us to accept the correct merges.

The first object prior we use is that humans perceive the world in terms of objects, or groups of percepts that behave similarly across time and tend to maintain their shape and size (Spelke 1990). We incorporate this prior by developing an *object representation objective*, which scores a proposed object representation based on how well it enables modelling observed dynamics, rewards, and estimated value. Behavioral consistency is implicit in objective: models of objects that change behavior over time will suffer from distribution shift and tend to be worse than models of objects with

consistent behavior. We use our objective to merge tracklets from standard segmentation and tracking algorithms together into a succinct set of object tracks (Figure 1). This allows us to infer object representations based on object dynamics, reward, and value rather than just appearance, improving visual robustness and connecting our object representation inference to relevance on specific tasks.

Learning causality in sparse reward settings is a fundamental challenge in reinforcement learning. The second human object prior we use is that objects interact only when contacting (Spelke 1990). We implement this prior by defining an object-contact state representation and reward and value approximation architecture. We represent the relationship between two objects by their relative position, velocity, acceleration, and whether they are contacting. This representation is both compact and sparse. We model reward and estimated value as a function of the pairwise features between contacting objects, enforcing the notion that objects interact only when contacting.

We combine our object inference, object state representation, and contact-centric estimation architectures to create an Object-Level Reinforcement Learner (OLRL). We compare OLRL with humans, standard deep reinforcement learning algorithms on MuJoCo (Todorov, Erez, and Tassa 2012) and Atari (Machado et al. 2018) environments, and show that it yields large improvements in sample and computational efficiency. Currently deep reinforcement learning research is often resource and time intensive due to the huge number of experiences needed. Our object detection and tracking module can be used as a general preprocessor for reinforcement learning, greatly increasing the pace and sample efficiency of experiments in this area.

In summary, our contributions are:

- An object representation objective function that encourages inference of objects with consistent behavior and high explanatory power of observed dynamics and rewards.
- A flexible reward and value estimation architecture that encodes the causality of object contacts.
- An object-centric RL agent that is orders of magnitude more sample efficient than standard deep RL algorithms and highly robust to visual changes.

Related Work

There has been much work on model-based deep reinforcement learning and predicting future states or values with deep networks. (Oh et al. 2015; Chiappa et al. 2017) use deep neural networks to accurately predict Atari frames hundreds of steps into the future. However, these works rely on hundreds of thousands of training frames and computationally intensive deep architectures, do not consider environment stochasticity, and predict at the pixel level rather than the more efficient object level. (Kaiser et al. 2019) integrate similar pixel-level frame prediction for Atari into a deep RL agent. (Garnelo, Arulkumaran, and Shanahan 2016) use reinforcement learning on a high-level symbolic world representation learned with no supervision, but must still learn what good world representations are and are only successful

on very simple environments. (Xue et al. 2016; Ebert et al. 2017; Oh, Singh, and Lee 2017; Higuera, Meger, and Dudek 2018) all learn to predict future state, but still predict either very low-level features that are difficult to learn on or high-level features that require many samples to effectively model.

Reward shaping is one way to incorporate human priors into reinforcement learning (Ng, Harada, and Russell 1999). Hybrid Reward Architectures (Van Seijen et al. 2017) show the potential of object-level reinforcement learning by using per-object reward functions to achieve up to 400x the score of Rainbow (Hessel et al. 2018), a state-of-the-art model-free agent, but rely on humans to label objects in its domain, Ms. Pacman.

Object state representations for reinforcement learning were proposed by (Diuk, Cohen, and Littman 2008) with a formal framework for describing and reasoning about object interactions. (Scholz et al. 2014) extended this framework with physics models of object dynamics. (Li, Sycara, and Iyer 2017) investigate integrating object information into modern deep learning approaches. (Kansky et al. 2017) learn more general probabilistic object models and demonstrate how to plan on such models using inference. By learning the parameters of physics-based environments models, (Woof and Chen 2018) develop an object embedding network to achieve great performance in complex environments. In contrast to our object recognition algorithm, all of these techniques require environment-specific object labels.

(Liang et al. 2016; Machado et al. 2018; Naddaf 2010) begin to tackle the problem of recognizing objects without extensive supervision or hand crafted, object specific recognition algorithms by introducing Blob-PROST, BASS, and DISCO, two large feature sets built by dividing the environment into grids and looking at monochrome blobs. Several recent works, MOREL (Goel, Weng, and Poupart 2018), OODP (Zhu, Huang, and Zhang 2018), IODINE (Greff et al. 2019), OP3 (Veerapaneni et al. 2019), ST-DIM (Anand et al. 2019), Transporter (Kulkarni et al. 2019), and SPACE (Lin et al. 2020) present unsupervised techniques for segmenting and modeling objects using deep neural networks. These works use the prior that the observed changes between successive frames can be explained by translations of groups of pixels. (Du et al. 2020) extends these works by using short-term motion cues to aid segmentation. In contrast to these works, we define object as having consistent dynamics, reward, and estimated value, rather than consistent appearance, making our representations more robust to visual perturbations and more task-relevant. In addition, we propose a flexible framework that uses existing segmentation and tracking algorithms, allowing for integration of powerful deep segmentation and tracking algorithms for applications to more realistic environments. Our object inference algorithm is not limited to a fixed number of object slots. For these reasons, our object representations are both more compact and are learned after hundreds, as opposed to tens or hundreds of thousands, of observations. Most critically, we develop an explicit object representation in terms of object positions, velocities, accelerations, and contacts and use this representation for our reinforcement learning.

Creswell et al. (2020) explores matching segmentations across time, optimizing a dynamics loss to do so. Luiten, Zulfikar, and Leibe (2020) uses a visual loss to match tracklets. This paper extends both of these works, connecting our object inference to reinforcement learning to optimize value and reward in addition to dynamics.

Background

Reinforcement learning solves the problem of taking actions in some environment to maximize some reward. Formally, let $a \in A$ be actions, $s \in S$ be environment states, $t \in 0, 1, \dots, \infty$ be time steps, $G(s', s, a) = P(s'|s, a)$ be a stochastic transition function, $R(s, a)$ be a stochastic reward function, and $\gamma \in [0, 1]$ be a discount factor. These define a Markov decision process where the goal at each time t is to take the action a_t that maximizes the expected discounted reward, $\sum_{t=0}^{\infty} R(s_t, a_t) \gamma^t$. Each observed (s, a, r, s') tuple is called an experience. Reinforcement learning solves this problem by learning a policy π which specifies the probability of the agent choosing each action given the current state. Define the state value function to be $V_\pi(s) = E_\pi[\sum_{k=0}^{\infty} \gamma^k R(s_{t+k}, a_{t+k}) | s_t = s]$ and the state-action value function to be $Q_\pi(s, a) = E_\pi[\sum_{k=0}^{\infty} \gamma^k R(s_{t+k}, a_{t+k}) | s_t = s, a_t = a]$, where $E_\pi[\cdot]$ denotes the expected value of the random variable given that the agent follows π . Then the optimal state value and state-action value functions are $V_*(s) = \max_\pi V_\pi(s)$ and $Q_*(s, a) = \max_\pi Q_\pi(s, a)$ for all $s \in S$ and $a \in A$, and an optimal policy π is one that is greedy with respect to the optimal state value or state-action value function.

In model-based reinforcement learning the agent learns a model of the world, and uses this model to plan actions to take or to simulate an environment to learn in. Specifically, the agent learns an approximation of $G(s', s, a)$, the transition function, and $R(s, a)$, the reward function. Intuitively, the better these models are, the better the resulting policy will be. One approach to improving these models is creating a better state representation. That is, rather than learn to predict the state and reward in terms of $s \in S$, learn a map into a smaller state space $h : S \rightarrow S'$, and learn models in this smaller state space. Intuitively, if $|S'|$ is much less than $|S|$ while preserving important features, better models can be learned with the same amount of experience. One general approach to this work is state aggregation (Bertsekas 2018), which examines when two states $s_1, s_2 \in S$ may be combined into a single state s_3 , creating a smaller state representation. For tasks where the observations are images or video, h is often thought of as a perception algorithm, processing images into meaningful visual features. Work in this area includes encoder-decoders (Oh et al. 2015; Xue et al. 2016; Ebert et al. 2017; Chiappa et al. 2017; Kaiser et al. 2019), object-like feature sets (Liang et al. 2016; Machado et al. 2018; Naddaf 2010), object keypoints (Kulkarni et al. 2019), and pixel masks of objects (Goel, Weng, and Poupart 2018; Zhu, Huang, and Zhang 2018; Veerapaneni et al. 2019; Greff et al. 2019; Anand et al. 2019; Lin et al. 2020; Du et al. 2020).

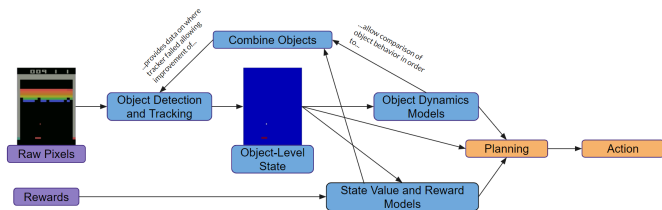


Figure 2: Diagram of OLRL framework

Object-Oriented RL Agent

Our object-level RL agent consists of three components. The first segments and tracks RGBD observations into tracklets, and then merges these tracklets into object tracks by optimizing an *object objective function* over maps from tracklets to tracks. The second component processes these object tracks into a small but descriptive object representation. The third component is a model-based, object-centric reinforcement algorithm that learns a policy using the object representation. Rather than extracting objects using visual losses, our agent jointly optimizes the object representation with the learned dynamics model and policy. By doing so, our object representation is grounded in task relevance and observed dynamics, and so is highly robust to visual noise and task-irrelevant distractors. Our approach is agnostic to the underlying segmentation and tracking algorithms used to produce the input tracklets and the model-based reinforcement learning algorithm used to learn a policy from the object representation. We give an overview of our OLRL agent in Figure 2.

Tracklets

Given T sequential RGBD observations of a d -dimensional environment as four-channel images $I \in \mathbb{R}^{T \times H \times W \times 4}$, our system first uses a tracking and segmentation algorithm \mathcal{S} to segment and track I into a set of tracklets L , where each tracklet $l \in \{0, 1\}^{T \times H \times W}$ is a set of instance masks (1 denoting part of the instance, 0 not) for each image observation. \mathcal{S} is tuned to oversegment and undertrack, so each tracklet contains at most one object with high confidence, but objects may be split across multiple tracklets.

Object Representation

We may represent objects by their contacts and absolute and relative position, velocity, and acceleration. Let K be a set of object tracks, where each track $k \in \{0, 1\}^{T \times H \times W}$ is the set of binary instance masks for each observation corresponding to an object. Thus, we represent the state at time t , o^t , by a tuple $(p_a, p_r, v_a, v_r, a_a, a_r, c)$ where $p_a, v_a, a_a \in \mathbb{R}^{|K|}$ are the absolute positions, velocities, and accelerations of objects, respectively and $p_r, v_r, a_r \in \mathbb{R}^{|K| \times (|K|-1)/2}$ are the relative positions, velocities, and accelerations between each pair of objects, respectively. Finally, $c \in \{0, 1\}^{|K| \times (|K|-1)/2}$ encodes contacts between object pairs. Positions, velocities, and accelerations are computed by taking the median of the observed object point cloud at each time, and contacts are computed from adjacency of object point clouds.

Object Objective

At the core of our object-oriented RL agent is our object objective function, which encodes our definition of objects as groups of percepts that maintains properties–dynamics, behavior–through time. Given a set of tracklets, agent actions, and rewards, our system merges tracklets to find a minimal set of objects that explain observed tracklet dynamics and agent rewards and have relevance to the learned task value function. Specifically, we seek to infer a map from tracklets to tracks, $M : l \in L \rightarrow k \in K$. Let o_M^T be the object representation of the observations using map M . We infer this map by defining an objective function to score candidate maps. Let $D : o_M^t, a^t \rightarrow [0, 1]^{d \times |K| \times |V_a|}$ be a probabilistic object velocity model over a discrete set of velocities V_d . Let $R : o_M^t, a^t \rightarrow r^t$ be an agent reward model, and $V : o_M^t, a^t \rightarrow v^t$ be an agent value model. Let $E_D(o_M^T, a^T)$, $E_R(o_M^T, a^T)$, and $E_V(o_M^T, a^T)$ be the errors of these models. Then our tracklet map objective function is

$$O(M) = E_D(o_M^T, a^T) + E_R(o_M^T, a^T) + E_V(o_M^T, a^T)$$

E_D , the dynamics error, is the mean expected absolute error of the velocity predictions:

$$E_D(o_M^T, a^T) = \frac{1}{|\hat{T}||T|} \sum_{t \in \hat{T}} D(o_M^t, a^t) \cdot |o_M^{t+1}[v_a] - V_d|$$

$o_M^{t+1}[v_a]$ is a $d \times |T|$ matrix of absolute velocities in the $t + 1$ th observation. We model pairwise reward, $R_{i,i'}$, and pairwise value, $V_{i,i'}$, a small 3-layer fully connected network. We use mean squared error for reward and value error

$$E_R(o_M^T, a^T) = \frac{1}{|\hat{T}|} \sum_{t \in \hat{T}} (R(o_M^t, a^t) - r^t)^2$$

$$E_V(o_M^T, a^T) = \frac{1}{|\hat{T}|} \sum_{t \in \hat{T}} (V(o_M^t, a^t) - v^t)^2$$

We seek the tracklet mapping M that minimizes this objective function.

$E_D(o_M^T, a^T)$, the error of the dynamics model, encodes that objects have consistent behavior across time. If two tracklets l_i and l'_i corresponding to different objects are mapped together, then the dynamics model will either have to average its predictions between the two objects or infer which object is present from recent dynamics, both of which will tend to increase predictive error. Conversely, if two tracklets l_i and l'_i corresponding to the same object are mapped together, then the dynamics model only needs to learn one model for both tracklets, instead of separate models for each, tending to decrease predictive error.

On similar principles, $E_R(o_M^T, a^T)$, the error of the reward model, and $E_V(o_M^T, a^T)$, the error of the value model, will tend to decrease when two tracklets corresponding to the same object are merged, but tend to increase when two tracklets corresponding to different objects are merged.

Since object positions, velocities, and accelerations are computed using the median of the object pointcloud position, merging tracklets into the background track will increase error by very little since the background point cloud is typically much larger than individual object point clouds. This is an important feature of this objective function: if an object has no task relevance, i.e. excluding it from the reward and value models does not increase predictive error and excluding it from the dynamics models does not increase predictive error on other task-relevant objects, then it will be merged with the background and effectively ignored by the agent. This allows inference of minimal, task-relevant object representations.

We initialize the set of tracks as the set of observed tracklets, $T = L$. We then greedily optimize our mapping M by choosing a random pair of candidate tracklets l_i, l'_i to map together, forming map M' , and accepting M' if $O(M') \leq O(M) + c$, where c is a regularization constant to encourage learning smaller object representations.

Object-Centric Reinforcement Learning

We propose a model-based reinforcement learning architecture motivated by the observation that objects tend to act on each other only when in contact (Spelke 1990). We model value and reward as a function of contacting objects and their relative features rather than learn to predict reward and value as a function of all object features, further reducing the dimensionality of our object representation. For computational efficiency, we only consider pairwise contacts. For an object pair i, i' , we define their pairwise features $o_{i,i'}$ as the relative position, velocity, and acceleration between i and i' and the absolute position, velocity, and acceleration of i and i' . Let $c(i, i') = 1$ if i and i' are contacting in the current observation and $n(i, i') = \sum_{i, i' \in M} c(i, i')$. Then we model reward and value as

$$R(o, a) = \frac{1}{n(i, i')} \sum_{i, i' \in M, c(i, i')=1} R_{i, i'}(o_{i, i'}, a)$$

$$V(o, a) = \frac{1}{n(i, i')} \sum_{i, i' \in M, c(i, i')=1} V_{i, i'}(o_{i, i'}, a)$$

Since we take the mean of the pairwise models, each can be independently trained to predict the observed rewards and estimated state-action values compute from them, allowing great flexibility when choosing the specific learning algorithms for each $R_{i, i'}$ and $V_{i, i'}$.

Our agent may then use the learned dynamics, reward, and value models to plan into the future and choose the action sequence with the highest predicted value. For a plan $p = \{o^0, o^1, \dots\}$ consisting of a set of predicted object states and corresponding action sequence $s_a = \{a_0, a_1, \dots\}$, the value is $Q(p, s_a) = \gamma^{|p|} V(o^{|p|}, a^{|p|}) + \sum_{t \in |p|} \gamma^t R(o^t, a^t)$.

Implementation

Segmentation and Tracking: We use UIOS (Xie et al. 2019), a pretrained RGBD instance segmentation network, to produce segmentations. To form tracklets, we match segments in adjacent observations by assigning each segment pair a

score based on visual similarity and physical proximity (see the Appendix for more details). We then greedily assign pairs with the lowest score below a certain threshold. Any unmatched segmentation is added as a new tracklet.

Object Objective Function: We model object dynamics by learning a probabilistic model of velocity. We first discretize velocity into $V_d = \{-30, \dots, 30\}$. We use an XGBoost (Chen and Guestrin 2016) tree for each object in each dimension to predict a probability vector over possible velocities for the object in the next time step. We choose a discrete model architecture over a continuous architecture to best model the often discontinuous outcomes of collisions, for example, elastic vs. perfectly inelastic behavior. We select a random 20% of observations to hold out for error computation as \hat{T} .

Model Based RL: We use on-policy Monte Carlo RL (Sutton and Barto 2018) to compute $Q(s, a)$ targets with $\gamma = 0.95$. Each time a new tracklet map is accepted, the agent retrains the dynamics, reward, and value models on the new object representation over past experiences. Actions are selected by planning two actions into the future and selecting the action that maximizes predicted expected value. Since our dynamics model outputs a probability over future states, we sample ten possible future states for each action path and take their mean value.

Experiments

We first evaluate our approach on a set of 3D environments with challenging confounding object behavior. We implement these environments in MuJoCo (Todorov, Erez, and Tassa 2012), a fast and realistic physics engine. Then we apply our object-centric agent to several Atari environments, and show that not only does it learn several orders of magnitude faster than classic Deep RL algorithms, but it also learns slightly faster than humans.

MuJoCo Environments: We propose a suite of custom 3D MuJoCo environments to highlight current challenges with learning object representations. The base tasks are controlling a tabletop agent to either gather or avoid moving objects, implemented by giving the agent a reward of +1 and -1, respectively, for contacting these objects. These tasks are deliberately quite simple, and easily solved by modern deep RL algorithms or segmented by current unsupervised segmentation algorithms. We introduce two *object randomization* tasks, gather+r and avoid+r, (Figure 3), where we randomize the color, size, and starting positions of the both the agent and reward objects after each episode, simulating changes in visual conditions or the objects themselves. The frequently changing object appearances confound existing unsupervised methods of learning object representations (Greff et al. 2019; Lin et al. 2020; Du et al. 2020) as they both rely primarily on visual cues to segment objects and can only represent a limited number of distinct objects.

In Figure 4 we compare the performance of our algorithm, OLRL, with A2C (Wu et al. 2017), and an agent that takes random actions. In addition, we show OLRL without tracklet mapping, OLRL-m. OLRL and OLRL-m are able to outperform A2C on the gather and avoid tasks with only 1/50th the experiences using our object representation and

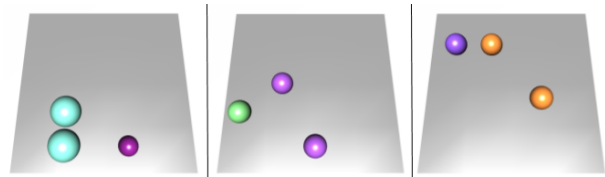


Figure 3: Starting configurations of three successive episodes of the tabletop MuJoCo tasks. The agent must control one ball to either gather or avoid the other balls.

	gather	avoid	gather+r	avoid+r
A2C	35.3 ± 4.2	-12.0 ± 3.7	38.0 ± 6.2	-15.7 ± 9.3
OLRL	103.3 ± 41.8	-17.7 ± 13.7	62.0 ± 3.7	-8.5 ± 7.3
OLRL-m	76.0 ± 55.0	-13.0 ± 6.0	34.7 ± 16.8	-25.3 ± 24.1
Random	29 ± 3.7	-20 ± 7.3	29.3 ± 7.6	-32.3 ± 15.0

Figure 4: Mean final episode scores on MuJoCo environments with standard deviations. A3C trained for 100,000 steps, OLRL trained for 2000.

contact-centric reward and value estimation architecture. On the gather+r and avoid+r tasks, both A2C and OLRL-m perform little better than random due to object appearance being randomized each episode, which prevents visual-based transfer of learned object properties from one episode to the next, essentially forcing these algorithms to start learning from scratch each episode. However, OLRL, by using our object objective function to reason about the behavior of objects, is able to quickly match new objects with past objects and associated value, reward, and dynamics models, as shown in Figure 5.

Atari Experiments: In this section we evaluate OLRL on several Atari games. The chosen Atari games present many challenging and general object inference problems, including distractor objects, large changes in orientation or observed size due to occlusion, visually identical but behaviorally different objects, and discontinuities in observed dynamics. Successfully segmenting, tracking, and succinctly representing these objects requires challenging reasoning over dynamics, reward, and value, which humans are able to do with ease, pointing to this reasoning being important and general beyond Atari. First we examine the object representations OLRL learns for each Atari game and point out several challenges OLRL was able to overcome by reasoning about dynamics and reward. Then we compare the performance of OLRL to standard deep RL algorithms, and finally we compare OLRL’s learning speed to that of human players. We use Felzenszwalb segmentation (Felzenszwalb and Huttenlocher 2004) rather than UOIS and treat all points as being at depth zero for our Atari results.

Object Inference Challenges: By using our object objective function to combine map tracklets together, we are able to rapidly infer succinct object representations of each of the games, as shown in Figure 6. Each game contains many *distractor objects*, which are visually distinct and even move but are of little for learning a policy. Specifically, each game has many colorful static background objects. More

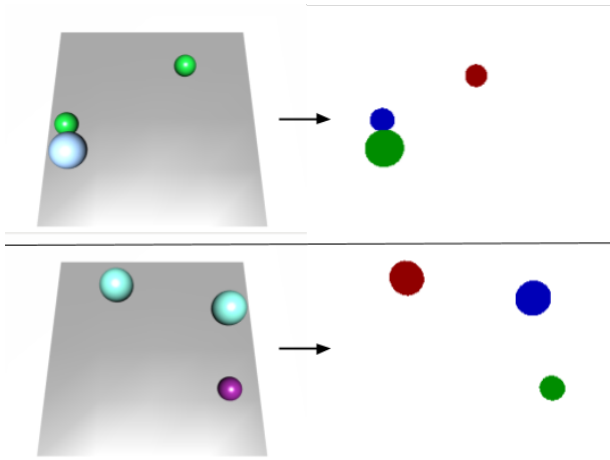


Figure 5: Left: RGB observation, Right: object segmentation. The top row is the segmentation at time $t=10$, and the bottom at $t=450$. By considering object dynamics and behavior, our system is able to map the agent controlled objects, light blue on top and purple on bottom, together, enabling transfer of past experiences.

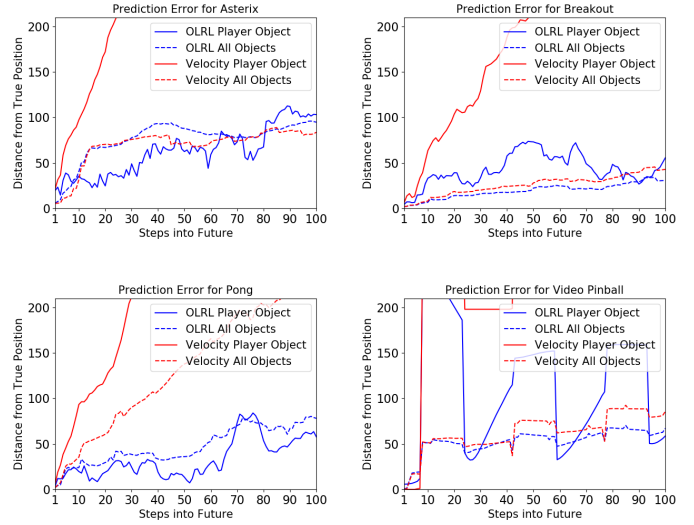


Figure 7: Model Error on Atari Environments. Distances are in pixels; for comparison, an Atari observation is 210×160 pixels.

challengingly, each game has a numerical score, and each numeral frequently appears and disappears, exhibiting distinct dynamics from the background. In three of the games, Asterix, Breakout, and Pong, the agent-controlled object frequently undergoes *changes in orientation or observed size* due to occlusion, rotating up to 180° or doubling or halving in size between successive observations, posing a challenge for any purely visual-based tracking algorithm. Finally, in two games, Asterix and Pong, there are task-irrelevant *objects that are visually identical or near-identical* to the agent-controlled object. This challenge is compounded by frequent *discontinuities in observed dynamics* when objects teleport large distances to starting positions during game resets: physical proximity and visual similarity together are insufficient to track them. OLRL is able to correctly segment and track objects through these challenges by relying on behavior to associate tracklets, ignoring task-irrelevant objects or associating visually distinct but behaviorally similar percepts together.

Dynamics Model Analysis: In this section we examine the speed and accuracy of our object-level perception and modeling. For each Atari game, we trained our model for only 2000 observations while playing random actions. We then evaluated our models by first playing n random actions, where n was sampled uniformly from $[50, 150]$, and then predicting the positions of objects for the next 100 steps. Figure 7 shows prediction error as the average distance between the predicted and actual object positions. Since many Atari objects do not move, we also show prediction error for the player-controlled object, which has complex dynamics. For the same reason, we use predicting constant object velocity as a natural baseline. Even with very little training data, our models have learned object dynamics with high accuracy tens of frames into the future, effective for short-term planning. In addition, model prediction error generally

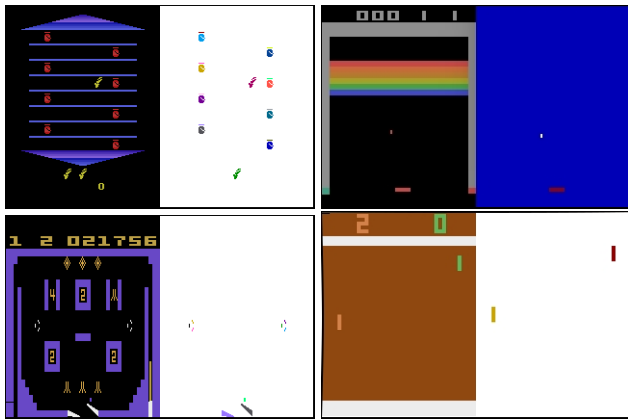


Figure 6: Object-level representations of Atari games. Clockwise from top left: Asterix, Breakout, Pong, and Video Pinball. Left: observed Atari game frames. Right: Inferred OLRL object segmentations

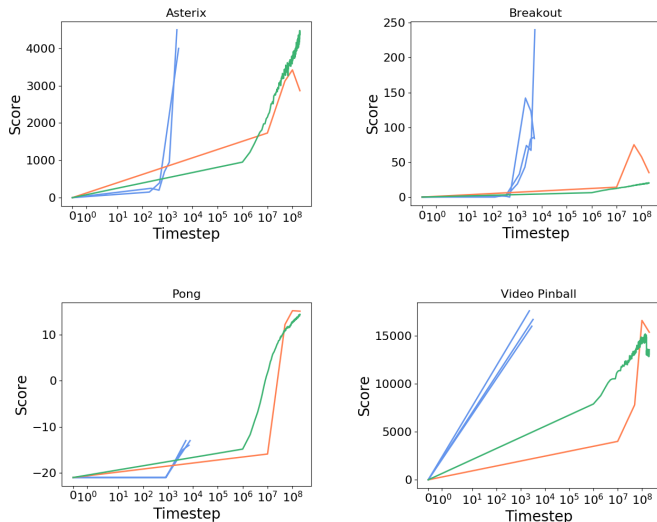


Figure 8: Comparison of OURL, DQN, and Blob-PROST. Blue: OURL, green: Blob-PROST, red: DQN. Note time steps are on log-scale.

does not explode for longer prediction horizons, allowing the agent to consider the approximate positions over objects even 100 steps into the future.

Comparison to Deep RL: We compare OURL to DQN and Blob-PROST in Figure 8. DQN and Blob-PROST data was drawn from (Machado et al. 2018). Our object-level agent reaches equivalent or greater performance than DQN and Blob-PROST with approximately 10,000x fewer experiences in three of the four Atari games. Although DQN and Blob-PROST outperform OURL in Pong, they require over 100x more experiences to reach the performance of OURL. Furthermore, SimPLe (Kaiser et al. 2019), the current state of the art for Atari in sample-limited regimes, achieves a mean of 54% the human-normalized score across Pong, Asterix, and Breakout after 100,000 steps; our agent achieves a mean of 176% human normalized score with fewer than 10,000 steps.

Comparison to Humans: We compare the maximum scores achieved by each time step for human players and OURL in Figure 9. For all games tested, this value plateaus for humans, indicating they are not increasing their highest score and have saturated learning. OURL learns faster than a human if OURL reaches a human’s maximum score in fewer time steps than that human. Despite humans having extensive prior knowledge, we find that OURL is able to exceed a human’s maximum score in fewer experiences than the human 55% of the time, demonstrating the power of the object representation and reinforcement learning we have designed. Details about human play data collection are in the Appendix.

Conclusion

In this paper, motivated by developmental psychology, we argue that objects should be defined primarily by behavioral,

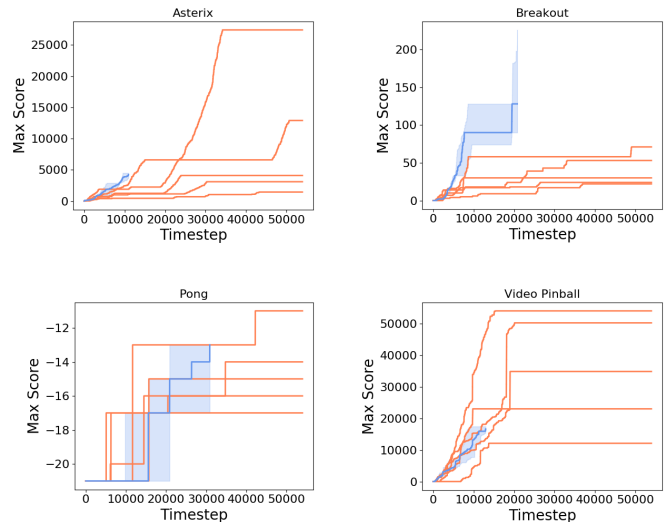


Figure 9: Comparison of OURL and human learning curves on Atari games. Each human learning curve shown in red. Median OURL score and error bars shown in blue.

rather than just visual, consistency across time. We formalize this notion into an object objective function and optimization algorithm which quickly infers minimal and task-relevant sets of objects with consistent dynamics, value, and reward. We further propose a flexible reward and value estimation architecture that encodes the causality of object contacts. We show that our object-level RL agent learns orders of magnitude faster than standard deep RL algorithms in 2D and 3D environments presenting a variety of realistic object inference challenges. Finally, our OURL approach is highly modular, adaptable to different segmentation, tracking, reinforcement learning, and sequence modelling algorithms.

This paper presents several future avenues of research. At the core of our OURL agent is the object objective function based off of model errors, which could be improved by integrating a more rigorous measurement of model error and uncertainty, taking into account training and test set sizes, for example. In addition, optimizing our object objective function requires expensive training of new dynamics, reward, and value models for each candidate representation and a large memory footprint to store all past experiences, limiting the number of steps we are able to train our OURL agent for. We hope that our OURL framework and grounding of objectness in behavior will serve as a foundation for further advancements in this area.

Acknowledgements

This work was supported by an NDSEG Fellowship and ONR grant N00014-18-1-2826. The GPU machine used for this research was donated by Nvidia.

References

- Anand, A.; Racah, E.; Ozair, S.; Bengio, Y.; Côté, M.-A.; and Hjelm, R. D. 2019. Unsupervised state representation learning in atari. In *Advances in Neural Information Processing Systems*, 8766–8779.
- Bertsekas, D. P. 2018. Feature-based aggregation and deep reinforcement learning: A survey and some new implementations. *IEEE/CAA Journal of Automatica Sinica* 6(1): 1–31.
- Brockman, G.; Cheung, V.; Pettersson, L.; Schneider, J.; Schulman, J.; Tang, J.; and Zaremba, W. 2016. OpenAI Gym.
- Chen, T.; and Guestrin, C. 2016. XGBoost: A Scalable Tree Boosting System. In *Proceedings of the 22nd ACM SIGKDD International Conference on Knowledge Discovery and Data Mining*, 785–794. ACM.
- Chiappa, S.; Racaniere, S.; Wierstra, D.; and Mohamed, S. 2017. Recurrent Environment Simulators. *arXiv:1704.02254*.
- Creswell, A.; Nikiforou, K.; Vinyals, O.; Saraiva, A.; Kabra, R.; Matthey, L.; Burgess, C.; Reynolds, M.; Tanburn, R.; Garnelo, M.; et al. 2020. AlignNet: Unsupervised Entity Alignment. *arXiv preprint arXiv:2007.08973*.
- Diuk, C.; Cohen, A.; and Littman, M. L. 2008. An Object-Oriented Representation for Efficient Reinforcement Learning. In *International Conference on Machine Learning*, 240–247. ACM.
- Du, Y.; Smith, K.; Uelman, T.; Tenenbaum, J.; and Wu, J. 2020. Unsupervised Discovery of 3D Physical Objects from Video. *arXiv preprint arXiv:2007.12348*.
- Ebert, F.; Finn, C.; Lee, A. X.; and Levine, S. 2017. Self-Supervised Visual Planning with Temporal Skip Connections. In *Conference on Robot Learning*, 344–356.
- Felzenszwalb, P. F.; and Huttenlocher, D. P. 2004. Efficient Graph-Based Image Segmentation. *International journal of computer vision* 59(2): 167–181.
- Garnelo, M.; Arulkumaran, K.; and Shanahan, M. 2016. Towards Deep Symbolic Reinforcement Learning. *arXiv:1609.05518*.
- Goel, V.; Weng, J.; and Poupart, P. 2018. Unsupervised Video Object Segmentation for Deep Reinforcement Learning. In *Advances in Neural Information Processing Systems*, 5688–5699.
- Greff, K.; Kaufmann, R. L.; Kabra, R.; Watters, N.; Burgess, C.; Zoran, D.; Matthey, L.; Botvinick, M.; and Lerchner, A. 2019. Multi-Object Representation Learning with Iterative Variational Inference. *arXiv preprint arXiv:1903.00450*.
- Hessel, M.; Modayil, J.; Van Hasselt, H.; Schaul, T.; Ostrovski, G.; Dabney, W.; Horgan, D.; Piot, B.; Azar, M.; and Silver, D. 2018. Rainbow: Combining Improvements in Deep Reinforcement Learning. In *Thirty-Second AAAI Conference on Artificial Intelligence*.
- Higuera, J. C. G.; Meger, D.; and Dudek, G. 2018. Synthesizing Neural Network Controllers with Probabilistic Model-Based Reinforcement Learning. In *2018 IEEE/RSJ International Conference on Intelligent Robots and Systems (IROS)*, 2538–2544. IEEE.
- Kaiser, L.; Babaeizadeh, M.; Milos, P.; Osinski, B.; Campbell, R. H.; Czechowski, K.; Erhan, D.; Finn, C.; Koza-kowski, P.; Levine, S.; et al. 2019. Model-Based Reinforcement Learning for Atari. *arXiv preprint arXiv:1903.00374*.
- Kansky, K.; Silver, T.; Mely, D. A.; Eldawy, M.; Lázaro-Gredilla, M.; Lou, X.; Dorfman, N.; Sidor, S.; Phoenix, S.; and George, D. 2017. Schema Networks: Zero-shot Transfer with a Generative Causal Model of Intuitive Physics. In *International Conference on Machine Learning*, 1809–1818.
- Ke, G.; Meng, Q.; Finley, T.; Wang, T.; Chen, W.; Ma, W.; Ye, Q.; and Liu, T.-Y. 2017. LightGBM: A Highly Efficient Gradient Boosting Decision Tree. In *Advances in Neural Information Processing Systems*, 3146–3154.
- Khotanzad, A.; and Hong, Y. H. 1990. Invariant Image Recognition by Zernike Moments. *IEEE Transactions on Pattern Analysis and Machine Intelligence* 12(5): 489–497.
- Kulkarni, T. D.; Gupta, A.; Ionescu, C.; Borgeaud, S.; Reynolds, M.; Zisserman, A.; and Mnih, V. 2019. Unsupervised learning of object keypoints for perception and control. In *Advances in Neural Information Processing Systems*, 10723–10733.
- Li, Y.; Sycara, K.; and Iyer, R. 2017. Object-Sensitive Deep Reinforcement Learning. *EPIc Series in Computing* 50: 20–35.
- Liang, Y.; Machado, M. C.; Talvitie, E.; and Bowling, M. 2016. State of the Art Control of Atari Games using Shallow Reinforcement Learning. In *Proceedings of the 2016 International Conference on Autonomous Agents & Multi-agent Systems*, 485–493. International Foundation for Autonomous Agents and Multiagent Systems.
- Lin, Z.; Wu, Y.-F.; Peri, S. V.; Sun, W.; Singh, G.; Deng, F.; Jiang, J.; and Ahn, S. 2020. SPACE: Unsupervised Object-Oriented Scene Representation via Spatial Attention and Decomposition. *arXiv preprint arXiv:2001.02407*.
- Luiten, J.; Zulfikar, I. E.; and Leibe, B. 2020. Unovost: Unsupervised offline video object segmentation and tracking. In *The IEEE Winter Conference on Applications of Computer Vision*, 2000–2009.
- Machado, M. C.; Bellemare, M. G.; Talvitie, E.; Veness, J.; Hausknecht, M.; and Bowling, M. 2018. Revisiting the Arcade Learning Environment: Evaluation Protocols and Open Problems for General Agents. *Journal of Artificial Intelligence Research* 61: 523–562.
- Mnih, V.; Badia, A. P.; Mirza, M.; Graves, A.; Lillicrap, T.; Harley, T.; Silver, D.; and Kavukcuoglu, K. 2016. Asynchronous Methods for Deep Reinforcement Learning. In *International Conference on Machine Learning*, 1928–1937.
- Mnih, V.; Kavukcuoglu, K.; Silver, D.; Rusu, A. A.; Veness, J.; Bellemare, M. G.; Graves, A.; Riedmiller, M.; Fidjeland, A. K.; Ostrovski, G.; et al. 2015. Human-Level Control through Deep Reinforcement Learning. *Nature* 518(7540): 529.

Naddaf, Y. 2010. *Game-independent AI Agents for Playing Atari 2600 Console Games*. Master’s thesis, University of Alberta.

Ng, A. Y.; Harada, D.; and Russell, S. 1999. Policy Invariance Under Reward Transformations: Theory and Application to Reward Shaping. In *International Conference on Machine Learning*.

Oh, J.; Guo, X.; Lee, H.; Lewis, R. L.; and Singh, S. 2015. Action-Conditional Video Prediction Using Deep Networks in Atari Games. In *Advances in Neural Information Processing Systems*, 2863–2871.

Oh, J.; Singh, S.; and Lee, H. 2017. Value Prediction Network. In *Advances in Neural Information Processing Systems*, 6120–6130.

Scholz, J.; Levihn, M.; Isbell, C.; and Wingate, D. 2014. A Physics-Based Model Prior for Object-Oriented MDPs. In *International Conference on Machine Learning*, 1089–1097.

Silver, D.; Schrittwieser, J.; Simonyan, K.; Antonoglou, I.; Huang, A.; Guez, A.; Hubert, T.; Baker, L.; Lai, M.; Bolton, A.; et al. 2017. Mastering the Game of Go without Human Knowledge. *Nature* 550(7676): 354.

Spelke, E. S. 1990. Principles of Object perception. *Cognitive Science* 14(1): 29–56.

Sutton, R. S. 1988. Learning to Predict by the Methods of Temporal Differences. *Machine Learning* 3(1): 9–44.

Sutton, R. S.; and Barto, A. G. 2018. *Reinforcement learning: An introduction*. MIT press.

Todorov, E.; Erez, T.; and Tassa, Y. 2012. Mujoco: A physics engine for model-based control. In *2012 IEEE/RSJ International Conference on Intelligent Robots and Systems*, 5026–5033. IEEE.

Van Seijen, H.; Fatemi, M.; Romoff, J.; Laroché, R.; Barnes, T.; and Tsang, J. 2017. Hybrid Reward Architecture for Reinforcement Learning. In *Advances in Neural Information Processing Systems*, 5392–5402.

Veerapaneni, R.; Co-Reyes, J. D.; Chang, M.; Janner, M.; Finn, C.; Wu, J.; Tenenbaum, J. B.; and Levine, S. 2019. Entity Abstraction in Visual Model-Based Reinforcement Learning. *arXiv preprint arXiv:1910.12827*.

Woof, W.; and Chen, K. 2018. Learning to Play General Video-Games via an Object Embedding Network. In *2018 IEEE Conference on Computational Intelligence and Games (CIG)*, 1–8. IEEE.

Wu, Y.; Mansimov, E.; Grosse, R. B.; Liao, S.; and Ba, J. 2017. Scalable trust-region method for deep reinforcement learning using kronecker-factored approximation. In *Advances in neural information processing systems*, 5279–5288.

Xie, C.; Xiang, Y.; Mousavian, A.; and Fox, D. 2019. The best of both modes: Separately leveraging rgb and depth for unseen object instance segmentation. In *Conference on Robot Learning (CoRL)*.

Xue, T.; Wu, J.; Bouman, K.; and Freeman, B. 2016. Visual Dynamics: Probabilistic Future Frame Synthesis via Cross Convolutional Networks. In *Advances in Neural Information Processing Systems*, 91–99.

Zhu, G.; Huang, Z.; and Zhang, C. 2018. Object-Oriented Dynamics Predictor. In Bengio, S.; Wallach, H.; Larochelle, H.; Grauman, K.; Cesa-Bianchi, N.; and Garnett, R., eds., *Advances in Neural Information Processing Systems 31*, 9804–9815. Curran Associates, Inc.

Implementation Details

Creating Tracklets

OORL uses a tracking and segmentation algorithm \mathbb{S} to process observations into tracklets, or tracked image segmentations. We only require that \mathbb{S} oversegment and undertrack, that is, never map two objects onto the same tracklet. OORL then learns a mapping from tracklets to tracks to form a compact and task specific object representation. The oversegmentation and undertracking requirement is generally easily met by tuning confidence thresholds; OORL is compatible with a wide variety of segmentation and tracking algorithms. We implement \mathbb{S} by using one of two segmentation algorithms to first oversegment each observation, and then a feature-based tracking algorithm to greedily match successive segmentations into tracklets.

Segmentation: For 3D environments, we use UOIS (Xie et al. 2019), a state of the art deep neural network for unseen object segmentation. For 2D environments, we use Felzenszwalb segmentation (Felzenszwalb and Huttenlocher 2004), a classical segmentation algorithm. Successfully using both a classical segmentation algorithm and a state of the art segmentation DNN demonstrates the flexibility of our framework. For UOIS, we set the `skip_pixels` to encourage oversegmentation. For Felzenszwalb segmentation, we use a scale of 1000 and sigma of 0 to encourage oversegmentation.

Tracking: We form tracklets by matching segmentations in successive observations to existing tracklets. Let L_{-1} be the set of existing tracklets in their most recently observed position at time t , so each tracklet $l_{-1} \in L_{-1}$ is a $\{0, 1\}^{\times H \times W}$ segmentation. Let S_{t+1} be the segmentations for observations at time $t + 1$, where each segmentation $s \in \{0, 1\}^{V \times H \times W}$. Given a tracklet and segmentation, $l_{-1} \in L_{-1}$ and $s_{t+1} \in S_{t+1}$, we assign a scalar tracking error $T(l_{-1}, s_{t+1})$ to the segmentation pair. We then greedily match segmentations to tracklets with the lowest error below a certain threshold t_e . Unmatched segmentations are added as new tracklets.

We use an ensemble of human-inspired tracking features for T , detailed in Equation 1.

$$T(l_{-1}, s_{t+1}) = w_0 \mathcal{F}_{disp}(l_{-1}, s_{t+1}) + w_1 \mathcal{F}_{shape}(l_{-1}, s_{t+1}) + w_2 \mathcal{F}_{disp}(l_{-1}, s_{t+1}) \mathcal{F}_{shape}(l_{-1}, s_{t+1}) + w_3 \mathcal{F}_{perm}(l_{-1}, s_{t+1}) + w_4 \mathcal{F}_{size}(l_{-1}, s_{t+1}) + w_5 \mathcal{F}_{motion}(l_{-1}, s_{t+1}) \quad (1)$$

$\mathcal{F}_{disp}(l_{-1}, s_{t+1})$ is the total change in relative distance between l_{-1} and s_{t+1} and all objects contacting s_{t+1} , cap-

turing the notion that over small changes in time the positions of objects generally do not change too much.

$$\mathcal{F}_{shape}(l_{-1}, s_{t+1}) = \sum_{i=1}^{25} |\log(Z_i(l_{-1})) - \log(Z_i(s_{t+1}))|$$

where $Z_i(o)$ = i th Zernike moment ((Khotanzad and Hong 1990)) of o , encoding object shape consistency.

$\mathcal{F}_{perm}(l_{-1}, s_{t+1})$ captures the intuition that objects generally do not appear or disappear and is the number of experiences since s_{t+1} was last seen,

$$\mathcal{F}_{size}(l_{-1}, s_{t+1}) = \max\left(\frac{|l_{-1}|}{|s_{t+1}|}, \frac{|s_{t+1}|}{|l_{-1}|}\right) - 1.$$

$\mathcal{F}_{motion}(l_{-1}, s_{t+1})$ encodes that many objects are background objects and are unlikely-move:

$$\mathcal{F}_{motion}(l_{-1}, s_{t+1}) = \log(\max(P_{motion}(l_{-1}, s_{t+1}), \epsilon)),$$

where ϵ is some small positive constant. Let

$$P_{motion}(l_{-1}, s_{t+1}) = P_{dm}(\text{Moves}(s_{t+1})|e_1, \dots, e_i)$$

if $med(l_{-1}) \neq med(s_{t+1})$, and

$$P_{motion}(l_{-1}, s_{t+1}) = P_{dm}(\text{NotMoves}(s_{t+1})|e_1, \dots, e_i)$$

if $med(l_{-1}) = med(s_{t+1})$. where $med(s)$ is the median coordinates of the observed point cloud composing segment s .

When we merge two tracklets l, l' during object inference, we discover an instance where the above segmentation algorithm has failed, as it should have tracked l to l' . We can use this information to learn a per-object tracking model. We learn tracking models consisting of two LightGBM (Ke et al. 2017) trees per object. We used LightGBM rather than XGBoost trees because of the large amount of tracking data made the faster training time of LightGBM advantageous. For each object, we trained a lightGBM tree on the negative tracking instances associated with that object and the tracking instance which were once negative but later learned to be positive via merging two tracklets into the object track. We used the tracking features described in Appendix A.1 as inputs. The LightGBM tree was trained to output $1 - P_t(l_{-1}, s_{t+1})$, where $P_t(l_{-1}, s_{t+1})$ is the probability l_{-1}, s_{t+1} are the same object. We form the learned tracking algorithm T_L , by taking the maximum of the base tracking algorithm T , and the learned LightGBM tracking algorithm.

Dynamics, Value, and Reward Models

Dynamics Models—We model the velocity of each object in each dimension with a separate XGBoost (Chen and Guestrin 2016) tree. Each tree outputs a probability vector over velocities, discretized in steps of 1 between -30 and 30. Each tree is trained to minimize multiclass logloss, has a maximum depth of $\max(2, \min(6, |D|/50))$, where D is the size of the training data. Experiences are split into a 80:20 train/validation split, which is used for early stopping of training (5 rounds), and for computing the model likelihoods used in the Infer algorithm in the main paper. Where

objects appear when they transition from not being present to being present is modelled with an XGBoost tree per object per dimension trained to output a probability vector over positions. Each tree has a maximum depth of 6 and is trained to minimize multiclass logloss, with a similar 80:20 train/validation data split. Object presence is modelled with an XGBoost tree per object, minimizing multiclass logloss on an 80:20 split with a maximum tree depth of 6. For all models, mean prediction was also evaluated, and if mean prediction yields better validation error it was used instead (we did this primarily to prevent objects with very little associated data from causing noisy validation error behavior in the XGBoost trees and interfering with the Infer algorithm).

Reward and Value Models—Our agent uses Monte Carlo Control (Sutton 1988) with a discount factor of 0.95 to estimate state-action values. We then learn to predict state-action reward and value with an XGBoost tree for each object pair. Each XGBoost tree trained to predict deviation from the mean value or reward given the absolute and relative positions, velocities, accelerations, and contact states of the object pair. Each tree was trained to predict the mean of a Gaussian distribution with variance 1 describing the reward distribution for each state-action \times object pair and trained to maximize likelihood. Data was split into 3:1 train/validation.

MuJoCo Environments

In this section we describe the parameters of our 3D MuJoCo environment suite.

environment	gather	avoid
number target objects	2	2
object shape	sphere	sphere
sphere radius	uniform(0.05, 0.1)	uniform(0.05, 0.1)
sphere color	uniform random	uniform random
agent speed	0.1	0.1
target object speed	0.2	0.05
target object contact reward	+1	-1
randomization	none	none

environment	gather+r	avoid+r
number target objects	2	2
object shape	sphere	sphere
sphere radius	uniform(0.05, 0.1)	uniform(0.05, 0.1)
sphere color	uniform random	uniform random
agent speed	0.1	0.1
target object speed	0.2	0.05
target object contact reward	+1	-1
randomization	color+size	color+size

Human Atari Learning Data

We conducted a study of human Atari game play for four games to obtain learning curves. Five participants were tasked with playing Asterix, Breakout, Pong, and Video Pinball for 15 minutes each. To ensure the environment the humans were tested on was identical to the environment we trained our agents on, we used OpenAI Gym (Brockman et al. 2016) as the Atari emulator. We found that there is

very high variance in score between participants, even on Asterix, which participants were unlikely to have played before. In every game at least one participant was able to beat the expert score in 15 minutes of play.